



DALHOUSIE UNIVERSITY

Retrieved from DalSpace, the institutional repository of
Dalhousie University

<https://dalspace.library.dal.ca/handle/10222/81728>

Version: Post-print

Publisher's version: Choi, H., Lake, C.B. and Hills, C.D. 2020. Particle size effects on
breakage of ACT aggregates under physical and environmental loadings

t. ASCE Journal of Hazardous, Toxic, and Radioactive Waste, 24(1): 04019029. DOI:
10.1061/%28ASCE%29HZ.2153-5515.0000468

1 **Particle Size Effects on Breakage of ACT Aggregates Under Physical and**
2 **Environmental Loadings**

3 Hun Choi¹, Craig B. Lake², and Colin D. Hills³

4
5
6
7
8
9
10
11
12
13

14 ¹ Former Graduate Student, Civil and Resource Engineering Department, Dalhousie
15 University, Canada.

16 ² Professor, Civil and Resource Engineering Department, Dalhousie University, Canada.

17 ³Professor, Centre for Contaminated Land Remediation, University of Greenwich,
18 United Kingdom; Adjunct Professor, Civil and Resource Engineering Department,
19 Dalhousie University, Canada

20

21

22 *Corresponding author: Craig B. Lake, Civil and Resource Engineering Department,
23 Dalhousie University, Halifax, Nova Scotia, Canada

24 E-mail: craig.lake@dal.ca, Tel.: +1 (902) 494 3220 Fax: +1 (902) 494 3108

25

26 **Abstract**

27 Aggregates manufactured from fine-grained thermal waste residues using accelerated
28 carbonation technology (ACT) represent a potential sustainable alternative to natural
29 aggregates. However, for these manufactured products to compete with virgin stone in
30 geotechnical applications, their durability under mechanical and environmental
31 loadings must be assessed. This paper describes particle breakage that occurs for
32 different grain sizes (entire sample, 5mm-2.5mm, and 2.5mm-1.25 mm) of a cement
33 kiln dust accelerated carbonated manufactured aggregate after undergoing triaxial
34 compression, triaxial shear and freeze/thaw (f/t) testing. It is shown that the particle
35 breakage of the aggregate is dominated by the larger (5mm-2.5mm) size fraction of the
36 sample under all loading conditions. Particle breakage results from f/t testing showed
37 that the 5mm-2.5mm size corresponded to similar or slightly less particle breakage than
38 that under triaxial shear, while the particle breakage of the 2.5mm-1.25mm aggregate
39 after 20 cycles of freeze-thaw was relatively small. The performance of the carbonated
40 aggregate in terms of relative breakage was similar or slightly better than natural
41 calcareous sand results in the literature.

42 **Keywords:** manufactured aggregate, particle breakage, accelerated carbonation,
43 compression, shear, freeze/thaw

44

45 **Introduction**

46 Sustainable aggregate manufacturing represents a potential solution to limited
47 aggregate supply in some geographical regions, and a sustainable waste management
48 solution for selected high-volume wastes currently landfilled. Challenging regulatory
49 approvals required for environmental permitting in developed countries also suggests
50 that manufactured aggregates will become increasingly important in the future. The use
51 of accelerated carbonation technology (ACT) has been shown to manufacture light-
52 weight aggregates from fine-grained thermal waste residuals while at the same time
53 sequestering CO₂ during the aggregate production process (Gunning et al. 2009). This
54 sustainability aspect of the aggregate has led to the development of ACT manufacturing
55 plants in the United Kingdom. Various researchers (e.g. Fernández et al. 2004;
56 Domingo et al. 2006; Costa et al. 2007) have described the science behind the ACT
57 process and it hence will not be repeated here.

58 Current application of ACT manufactured aggregates in the United Kingdom
59 is replacement aggregates for concrete blocks (Gunning et al. 2011). For these
60 aggregates to be used in broader applications such as engineered fill for roadway
61 construction, their sustained durability under mechanical and environmental loadings
62 is critical. The durability of coarse-grained soil particles in geotechnical applications
63 has been the subject of numerous studies in the literature due to concerns related to
64 particle breakage (i.e. large dams (Marsal 1967), deep foundations (Klotz & Coop
65 2001), roadways (Zheghal 2009) and petroleum applications (Zheng & Tannant 2016).
66 Work by Marsal (1967); Lee & Farhoomand (1967); Hardin (1985) represent examples
67 of early studies performed to investigate the durability of soil particles by examining
68 particle breakage. It has been shown in these, and other studies, that the amount of soil

69 particle breakage will depend, inter alia, on the individual soil particle's mineralogy,
70 shape, and size (Lee & Farhoomand 1967; Hardin 1985). Stress level, stress path, and
71 time effects (Coop 1990; Lade et al. 1996; Yamamuro & Lade 1993 Altuhafi & Coop
72 2011) also play key roles in particle breakage.

73 Reported ACT manufactured aggregate individual particle strengths are in the
74 order of 0.5 MPa to 1 MPa (Lake et al. 2016) and hence are potentially susceptible to
75 particle breakage, similar to weaker grain soil particles such as calcareous sands (e.g.
76 Coop 1990). As accelerated carbonated aggregates are commercially available and
77 being further developed, data on aggregate breakage under different loadings is needed
78 to elucidate potential applications outside of bound systems. Thus, the purpose of this
79 paper is to provide a relative comparison of particle breakage for an accelerated
80 carbonated aggregate developed from cement kiln dust previously described by Lake et
81 al. (2016). In this paper the manufactured aggregate is subjected to a series of triaxial
82 tests (drained isotropic compression and drained isotropic compression followed by
83 drained axial shear) as well as (f/t) tests. The influence of aggregate size/gradation on
84 the particle breakage is evaluated by examining changes in grain size distributions of
85 the samples by calculating relative breakage, as defined by Hardin (1985). Given that
86 the ACT manufacturing process can control the final size of the aggregate,
87 understanding the role of size in particle breakage is useful as a potential tool for
88 improving the durability performance of the product.

89

90 **Materials and Methods**

91 *Cement Kiln Dust ACT Aggregate Production Process*

92 The testing performed in this paper used a cement kiln dust (CKD) material previously

93 described by Lake et al. (2016). In summary, the material was obtained from a Lafarge
94 cement plant in Brookfield (Nova Scotia, Canada) in August 2014. The CKD consists
95 of calcium, iron, silica, aluminum, magnesium and potassium oxides, with 42% CaO
96 content being the key carbonate-able mineral in producing the aggregate.

97 The pelleting process for carbonated aggregate manufacturing described by
98 Lake et al. (2016) was modified slightly in an attempt to produce a stronger aggregate
99 than the ~ 1MPa strength from that work. Pelletizing involved pre-mixing 400g (dry
100 mass) of CKD with 130g of water using a laboratory paddle mixer. During this phase
101 of the mixing process, CKD with water was mixed for 45 to 60 seconds at a 50 rpm
102 mixing speed followed by 30 to 60 seconds at 120 rpm. Subsequently, an additional 60g
103 of CKD was added at a 120 rpm mixing speed and then 40g CKD was added to mixer;
104 then mixed for 30 seconds at 50 rpm to produce rounded aggregates. The mix was then
105 placed in a rotating drum with CO₂ saturation for 15 minutes at 50 rpm to complete the
106 process. The carbonated aggregates in this study were air-cured at $20 \pm 2^{\circ}\text{C}$ and ~25%
107 relative humidity conditions in a lab for at least 28 days prior to being subjected to any
108 testing. As reported by Lake et al. (2016), the relative density (i.e. specific gravity) of
109 the aggregates for this process is 2.1. When placed in a loose compaction state, the bulk
110 density is 1200 kg/m³.

111 In this paper, three different particle size distributions were assessed for
112 particle breakage. The entire particle size distribution produced from the ACT process,
113 referred to as “EPS” in this paper, was used initially for testing. Additional aggregate
114 was prepared using the same techniques for the EPS but after curing, the aggregate was
115 segregated into two distinct size fractions. This was accomplished by passing the
116 material through the 5 mm sieve, followed by the 2.5 mm sieve, followed by the 1.25

117 mm sieve. Material retained on the 5 mm sieve and passing the 1.25 mm sieve was
118 discarded. Material retained on the 2.5 mm sieve is referred to as the “5-2.5PS” sample
119 in this paper and the material retained on the 1.25 mm sieve is referred to as the “2.5-
120 1.25PS” sample.

121

122 *Aggregate Testing*

123 Single Aggregate Pellet Strength

124 To provide an initial assessment of individual particle strength, a single pellet
125 compressive strength test (ASTM D4179-11, 2011), as described by Lake et al. (2016)
126 was used. Ten (10) samples were taken from the two carbonated aggregate grain sizes
127 prepared (i.e. 5-2.5PS; 2.5-1.25PS) and subjected to single pellet compressive strength
128 tests. The mean value of the strength was reported. Particle strengths were measured at
129 7, 15 and 27 days of air-curing to allow comparison to aggregates presented by Lake et
130 al. (2016).

131

132 Drained Isotropic Triaxial Compression Tests

133 To assess the extent of particle breakage of the accelerated carbonated aggregate during
134 drained isotropic triaxial compression testing, the three grain sizes were subjected to
135 isotropic compression tests similar to that described by Lake et al. (2016). For the EPS
136 material, two subsamples were taken of the prepared aggregate for each test; one was
137 submitted to a grain size analysis and the second used in the triaxial compression tests.
138 For the compression tests, the given aggregate size was lightly compacted in a split
139 mould (70mm inside diameter x 150mm high) and subjected to saturation under 35 kPa
140 effective confining pressure in a triaxial cell. The sample was then subjected to

141 consolidation under the desired effective confining pressure (600, 800, 1000, 1200 or
142 1400 kPa) to produce the isotropic compression conditions desired. The 1400 kPa
143 represents the limit of the cell pressure available. The test progressed until the specimen
144 reached equilibrium in a drained state at the desired effective consolidation stress. After
145 this was achieved, the grain size curve (by dry weight) of the sample was determined
146 in order to assess the extent of particle breakage that occurred. For the 5-2.5PS and 2.5-
147 1.25PS material, only the grain size distributions after the compression tests were
148 performed. For all tests, the grain size distributions of samples before and after triaxial
149 testing were plotted and compared visually as well as calculating the relative breakage
150 of the particle using the method developed by Hardin (1985). Hardin (1985) assumed
151 that the breakage of particles terminated when the gradation curve of a soil reached a
152 stable condition (i.e. when the final condition achieved was when all particles were
153 smaller than 0.074 mm (sieve No. 200)). The relative breakage (B_r) of soil can then be
154 calculated from the following equation (Hardin, 1985):

$$155 \quad B_r = \frac{B_t}{B_p} \quad (1)$$

156 Where B_p is the breakage potential (calculated as the area between the original grain
157 size distribution curve and a vertical line drawn at the 0.074mm sieve size) and B_t is
158 the total breakage (calculated as the area between the initial and final grain size
159 distribution curves). A value of B_r of zero would mean there was no change in grain
160 size distribution (i.e. no breakage) during testing while a value of one would mean
161 that all particles (i.e. maximum breakage) were reduced to sizes less than 0.074 mm
162 size during testing. Readers can access good visual descriptions of the value B_r from
163 Hardin (1985).

164 Drained Isotropic Compression, Drained Axial Shear Triaxial Tests

165 To assess the extent of particle breakage of the carbonated aggregate under shearing
166 conditions, the three different particle size fractions (i.e. EPS, 5-2.5PS, 2.5-1.25PS)
167 were subjected to drained isotropic compression followed by drained axial shear.
168 Samples were prepared similarly to those described in the previous section. In summary,
169 the given aggregate size was lightly compacted in a split-mold and subjected to
170 saturation under an effective confining pressure of 35 kPa (ASTM 4767-11, 2011). The
171 sample was then subjected to consolidation under the desired effective confining
172 pressure (600, 800, 1000, 1200 or 1400 kPa) and then subsequently sheared under
173 drained conditions at an axial displacement rate of 1.5 mm/min. Axial loading was
174 terminated at 15% axial strain to provide a common strain level. Similar to the triaxial
175 compression tests described in the previous section, grain size distributions were
176 compared before and after testing and the relative breakage calculated.

177

178 Freeze/Thaw Durability Testing

179 F/t durability testing, similar to that described by Lake et al. (2016) was performed on
180 the three different carbonated aggregate sizes (i.e. EPS, 5-2.5PS, 2.5-1.25PS). To
181 summarize, the aggregate samples were soaked in water for 4 hours and then surface
182 dried for approximately 15min. The test aggregate samples were then subjected to 10
183 or 20 f/t cycles that included freezing to $-17.5 \pm 2.5^{\circ}\text{C}$ for 24h and then thawing in a
184 water bath at room temperature ($\sim 20 \pm 2^{\circ}\text{C}$) for 4h (BSI BS EN 13055-4, 2016). The
185 20 cycles is recommended in the standard referenced above while 10 cycles allowed an
186 examination of breakage at an intermediate step in the f/t process. At the end of the f/t
187 cycles, the samples were subjected to grain size analyses to compare particle size

188 distributions before and after the f/t cycling. For comparison to triaxial compression
189 and/or triaxial shear testing, relative breakage was calculated at the end of each test.

190

191 **Results**

192 *Single Aggregate Pellet Strength*

193 Particle strengths for the two sizes increased as the curing time increased. The 5-2.5PS
194 aggregate achieved strengths of 1.8 MPa, 2.6 MPa, and 2.9 MPa after 7, 15, and 27 days
195 of curing, respectively. The 2.5-1.25PS aggregate achieved strengths of 2.0 MPa,
196 2.8 MPa and 3.0 MPa after 7, 15, and 27 days of curing respectively. For these simple
197 particle strength tests, there appears to be little, if any, difference in particle strength
198 between the two particle sizes tested. These test results confirmed that the majority of
199 the aggregate curing was completed after 28 days.

200

201 *Drained Isotropic Triaxial Compression Testing*

202 EPS

203 Figure 1 shows the particle size distributions for the EPS size of accelerated carbonated
204 aggregate before and after the drained isotropic triaxial compression tests for the five
205 effective confining pressures employed (600, 800, 1000, 1200, and 1400 kPa). As
206 seen from Figure 1, the grain size distributions of the sample visually changed little
207 during these tests. At the higher confining pressures (1200 kPa and 1400 kPa), the grain
208 size did change slightly as is evident by the increase in the finer fraction of the soil. The
209 resulting relative breakage (B_r) values for the EPS size of ACT aggregate is shown on
210 the inset of Figure 1. Similar to the visual observations noted above, B_r increased as the
211 confining pressure increased; the greatest increase occurring from 1000 to 1200 kPa.

212 5-2.5PS

213 Figure 2 shows the particle size distributions for the ACT aggregate before and after
214 the drained isotropic triaxial compression testing for the 5-2.5PS material. The initial
215 particle size distribution is a straight line as there is only one particle size present in
216 this sample. As seen from Figure 2, the grain size distributions of the sample visually
217 changed more than that for the EPS during these tests. It appears when examining
218 these grain size plots that there is a more pronounced effect on particle crushing
219 compared to that of the entire grain size distribution and that as the confining pressure
220 increased, the breakage also appeared to increase (i.e. appearance of more finer grain
221 fraction in the sample). The resulting relative breakage for this size is shown on the
222 inset of Figure 2, and confirms this observation. It is also noted that the relative
223 breakage found for this aggregate size was higher than that of the EPS. This
224 observation of how larger particle size, and grain size uniformity can result in
225 increases in particle breakage is consistent with Cassini et al. (2013) and Altuhafi &
226 Coop (2011).

227

228 2.5-1.25PS

229 Figure 3 shows the particle size distributions for the accelerated carbonated aggregate
230 before and after the drained isotropic triaxial compression testing for the 2.5-1.25PS
231 material. As with the 5-2.5PS material, the initial particle size distribution is a straight
232 line as only one particle size is present in this sample. As seen from Figure 3, the grain
233 size distributions of the sample visually changed less than the 5-2.5PS sample and that
234 of the EPS during these tests. It also appears that there was some minor particle
235 breakage as the confining pressure increased. The resulting relative breakage for this

236 size as shown on the inset of Figure 3 confirms this observation. It is also noted that the
237 breakage parameters found for this size aggregate were lower than that of the EPS and
238 the 5mm-2.5mm sample. This is perhaps not surprising when comparing to the EPS as
239 it is likely most of the particle breakage occurred in the 5mm-2.5mm fraction of the
240 sample.

241

242 *Drained Isotropic Compression, Drained Axial Shear Triaxial Test*

243 EPS

244 Figure 4 shows the particle size distributions for the carbonated aggregate before and
245 after the drained triaxial shear testing for the EPS particle size distribution for the five
246 effective confining pressures employed (600, 800, 1000, 1200, and 1400 kPa). As
247 seen from Figure 4, compared to the isotropic triaxial compression tests for the EPS,
248 there was noticeably more particle breakage from the shear testing. There was also more
249 particle breakage as the confining pressure was increased. The resulting relative
250 breakages for the carbonated aggregates are shown on the inset of Figure 4. Similar to
251 the visual observations noted above, the relative breakage increased as the confining
252 pressure increased. Also to note is the higher values of B_r relative to the isotropic triaxial
253 compression tests reported in Figure 1. As will be discussed later, this is due to the
254 higher mean stress in the samples relative to isotropic triaxial compression tests and the
255 shear being generated in the samples.

256

257 5-2.5PS

258 Figure 5 shows the particle size distributions for the carbonated aggregate before and

259 after the drained triaxial shear testing for the 5-2.5PS material. As seen from Figure 5,
260 the grain size distributions of the sample visually changed more than that for the EPS
261 during these tests, similar to that observed for the isotropic triaxial compression tests.
262 It also appears when examining these grain size plots that there is a more pronounced
263 effect on particle crushing compared to that of the EPS and, that as the confining
264 pressure increased, there was the appearance of more of a finer grain fraction. The
265 resulting relative breakage for the carbonated aggregate, as shown on the inset of
266 Figure 5, confirms this observation. It is also noted that the B_r values found for this size
267 aggregate were higher than that of the EPS and that the values of B_r were higher than
268 that for the isotropic triaxial compression tests.

269

270 2.5-1.25PS

271 Figure 6 shows the particle size distributions for the 2.5-1.25PS carbonated aggregate
272 before and after the drained triaxial shear testing. As seen from Figure 6, the grain size
273 distributions of the samples for triaxial shear visually changed less than both the 5-
274 2.5PS sample and that of the EPS during these tests. It does visually appear that there
275 was some minor particle breakage as the confining pressure increased, albeit less than
276 the other two sizes. The resulting relative breakage (B_r) for the 2.5-1.25PS material, as
277 shown on the inset of Figure 6, confirms this observation. It is also noted that the
278 particle breakage found for this size aggregate was lower than that of the EPS and the
279 5mm-2.5mm sample. Also noted is the relative increase in B_r compared to triaxial
280 compression testing.

281

282 *Freeze/Thaw Cycle Effect on Particle Breakage*

283 Figure 7 shows the grain size distribution of the EPS before and after f/t cycle testing.
284 After 10 cycles of f/t it is apparent that the grain size distribution of the EPS has a finer
285 grain size distribution and after 20 cycles of f/t, this particle size became even finer.
286 The percent passing the 2.5 mm sieve has increased the most in both instances,
287 indicating the larger portion of the sample may be exhibiting more breakage. This
288 phenomenon of particle breakage of the larger size aggregate can be examined further
289 when examining the isolated sizes. The 5-2.5PS material exhibited significantly more
290 breakage than that of 2.5-1.25PS. The 2.5-1.25PS grain size curve visually changed
291 little.

292 Although particle breakage is usually for mechanical loading applications, it is
293 interesting to calculate B_r for the f/t cycle tests (see inset of Figure 7). The values of B_r
294 corresponded with the visual observations of the grain size curves (more breakage with
295 f/t cycles at 20 than 10; at a given f/t/ cycle, breakage increases
296 5-2.5PS>EPS>2.5-1.25PS).

297

298 **Discussion**

299 *Particle Breakage Comparison between Triaxial Compression, Triaxial Shear, and*
300 *Freeze/Thaw Testing*

301 It is useful to compare the particle breakage obtained from the triaxial compression,
302 triaxial shear, and f/t cycle testing to ascertain the effect that different loading conditions
303 would have on the particle breakage of the carbonated aggregate. Figure 8 shows the
304 values of B_r obtained from these three different test methods. For ease of comparison,
305 results are presented in terms of mean stress, ρ' ($\rho' = (\sigma'_1 + \sigma'_2 + \sigma'_3)/3$) where σ'_1 and σ'_3

306 ($\sigma'_2 = \sigma'_3$ for these triaxial tests) are the major principal effective stress (i.e. axial stress)
307 and minor principal stress (i.e. effective confining stress) at failure. Since triaxial
308 compression and triaxial shear tests were performed under the same effective confining
309 pressures, the use of mean stress, p' , allows the “additional” axial stress to be accounted
310 for when examining stresses. For the purpose of this paper, the mean stress at the end
311 of the 15% strain level (i.e. termination of the test) was used. It should also be noted
312 that the f/t tests were performed under “zero external mean stress” conditions and hence
313 the grey shading observed on Figure 8 represents the range of B_r values for the 10 and
314 20 f/t cycles for each particle size.

315

316 As previously discussed, it is apparent that for the various triaxial tests, the
317 influence of shear resulted in the highest amount of particle breakage (i.e. when
318 comparing similar mean stresses). As discussed by Coop (1990), the true measure of
319 particle breakage is obtained from critical state conditions (which were not reached in
320 these tests) and hence this must be remembered when examining these test results.

321 It is noted that for a given loading condition, the 5-2.5PS aggregate underwent more
322 relative breakage (B_r) than that of the 2.5-1.25PS aggregate. When one examines the f/t
323 cycle testing results relative to the triaxial compression and triaxial shear results, it is
324 interesting to see that the particle breakage from f/t cycle testing for the EPS and
325 5mm-2.5mm size corresponds to much higher particle breakage than triaxial
326 compression (for similar particle sizes) testing but similar to slightly lower particle
327 breakage as that under triaxial shear. This suggests that environmental factors such as
328 f/t cycle may be just as important a design consideration for the ACT aggregate as that
329 compared to loading conditions. In contrast, the particle breakage of the 2.5-1.25PS

330 aggregate after 20 cycles of f/t is relatively small and similar in magnitude to the same
331 size aggregate under triaxial compression test conditions.

332

333 *Comparison of ACT Aggregate Particle Breakage to Other Studies*

334 Even though there are many different approaches to assessing particle breakage in the
335 literature, it is useful to try, at least from a qualitative standpoint, to compare particle
336 breakage obtained from this study to that of previous studies. For the purposes of this
337 study, calcareous sands studied by Shipton & Coop (2012) (using data from
338 Coop (1990)) and Shahnazari & Rezvani (2013) as well as predominantly silica sands
339 tested by Mun & McCartney (2017) are used as reference materials. The silica sand
340 tested by Mun & McCartney (2017) is relatively durable compared to the calcareous
341 sands tested by Coop and his coworkers. These two types of materials represent natural
342 aggregates, both used in construction applications.

343

344 For this research, some values for B_r for other studies were estimated visually from
345 plots and hence this may lead to some discrepancy. However, from a qualitative
346 perspective, approximations were deemed sufficient. Also to note is that the results of
347 Shipton & Coop (2012) and some of Shahnazari & Rezvani (2013) were a mix of
348 isotropic compression tests and drained triaxial shear tests. As well, the tests by Shipton
349 & Coop (2012) were run to higher strain levels than this study (i.e. would account for
350 more particle breakage).

351 Figure 9 shows B_r values for the various studies. Also shown on Figure 9 are
352 the results for the 5-2.5PS aggregate and the 2.5-1.25PS aggregate in this study. The
353 results of the EPS in this study always fell between these two samples and hence are

354 not included on Figure 9 for clarity purposes. As shown on Figure 9, at a given B_r , it
355 took significantly more mean stress for Mun and McCartney (2017) to achieve the same
356 particle breakage as compared to the ACT aggregate in this study. This is not surprising
357 given the relative differences in mineralogy and individual particle strengths of the
358 aggregates. If one compares the ACT manufactured aggregate to the natural calcareous
359 sand results for similar values of B_r it can be seen that similar or less mean stress is
360 required to achieve a similar particle breakage as that in this study. This is somewhat
361 encouraging in that calcareous sands have shown to be adequate materials for
362 construction projects in geotechnical applications provided loading and/or strain level
363 is limited to control particle breakage.

364

365 *Implication for Qualitative Manufacturing of ACT Aggregates*

366 There are several practical implications from this work related to ACT aggregate
367 manufacturing. Firstly, it is apparent that similar to other particle breakage studies in
368 the literature, larger particle sizes (i.e. 5-2.5PS size fraction in this study) are more
369 susceptible to particle breakage relative to smaller size particles (2.5-1.25PS). This
370 suggests that if aggregates manufactured by ACT as in this study were to be used in
371 geotechnical applications in which they will be subjected to shear and/or compression
372 conditions where the mean stresses approached or exceeded those in this research,
373 aggregates in the 2.5-1.25PS size range would perform better than those in the 5 mm-
374 2.5mm range. Given that the particle sizes can be controlled in the commercial
375 aggregate manufacturing process, a move to smaller particles may be preferred in
376 geotechnical applications, especially those in shear applications (i.e. roadways,
377 embankment slopes). If the aggregate is to be used in applications where shear is limited

378 and loading is predominately isotropic compression, then the amount of particle
379 breakage is expected to be small (e.g. wide fills). For example, for the 2.5-1.25PS size,
380 B_r values were less than 0.01 for mean stresses up to 1400 kPa in triaxial compression
381 tests. This stress range would be above most common stress applications for urban
382 developments.

383

384 *Exposure to Freeze/Thaw Cycling*

385 As shown in Figure 8, for f/t cycle tests carried out to only 20 cycles, resultant relative
386 breakage was at or near that from the triaxial shear tests for the 2.5-1.25PS carbonated
387 aggregate. This suggests that care should be taken to ensure exposure to f/t cycles is
388 limited for this size of aggregate. However, the f/t performance of the 2.5-1.25PS size
389 was significantly better than that of the 5-2.5PS size. For the 20 f/t cycles, limited
390 breakage was observed. This observation should be taken within the context that 20 f/t
391 cycles may not be representative of field applications (i.e. more f/t cycles may be
392 present in the field). This is an area in which further testing would be useful. The
393 manufacturing of carbonated aggregates smaller than 2.5mm appears to be desirable if
394 f/t is a concern.

395

396 **Summary and Conclusions**

397 This paper has presented the results of various tests designed to examine the amount of
398 particle breakage that occurs for the CKD-derived accelerated carbonated aggregate
399 developed in this study. Of particular emphasis in this study is the role of particle size
400 on relative breakage (B_r) for the aggregate product. Triaxial compression, triaxial shear
401 and f/t cycling tests were performed on the carbonated aggregate using the entire grain

402 size distribution and with isolated particle sizes (5-2.5PS and 2.5-1.25PS) to assess
403 particle breakage. The grain sizes before and after testing were used to calculate the
404 relative breakage, B_r . This parameter provides a fairly simple technique to provide
405 relative comparisons between grain sizes and also allows comparisons to be made with
406 previous studies related to calcareous sands and other more durable sands.

407 It was shown in this study that similar to other studies in the literature for
408 natural soils, the majority of particle breakage in the accelerated carbonated aggregate
409 occurred in the large particle size (5-2.5PS) relative to the smaller particle size (2.5-
410 1.25PS). This observation was present regardless of the test method performed.

411 Particle breakage results from f/t testing showed that the EPS and 5-2.5PS
412 materials corresponded to similar or slightly less particle breakage as that under triaxial
413 shear. This suggests that environmental factors such as f/t may be as important a
414 consideration in application to loading conditions. In contrast, the particle breakage of
415 the 2.5-1.25PS material after 20 cycles of f/t was small and similar in magnitude to the
416 same size aggregate under low to medium confining pressures for triaxial compression.
417 The performance of the accelerated carbonated aggregate in terms of relative breakage
418 (i.e. B_r) was similar or slightly better than natural calcareous sand results found in the
419 literature but substantially higher than more durable mineral fraction sands. This is an
420 interesting finding in that calcareous sands, although not the most desirable sand to use
421 in construction, can be used when its geotechnical limits are known and loads and
422 strains are limited to account for this performance. More work is required to examine
423 these limited conditions for the accelerated carbonated aggregate, especially at higher
424 strain levels and higher levels of f/t performance.

425

426

427

428

429

430

431

432

433

434

435

436

437

438

439

440

441

442

443

444

445 **Figure Captions**

446

447 Fig. 1. Particle size distributions for the EPS ACT aggregate sample before and after
448 triaxial compression.

449 Fig. 2. Particle size distributions for the 5-2.5PS ACT aggregate sample before and after
450 triaxial compression.

451 Fig. 3. Particle size distributions for the 2.5-1.25PS ACT aggregate sample before and
452 after triaxial compression.

453 Fig. 4. Particle size distributions for the entire size ACT aggregate sample before and
454 after triaxial shear.

455 Fig. 5. Particle size distributions for the 5-2.5PS ACT aggregate sample before and after
456 triaxial shear.

457 Fig. 6. Particle size distributions for the 2.5-1.25PS ACT aggregate sample before and
458 after triaxial shear.

459 Fig. 7. ACT aggregate particle size distributions, before and after 10 and 20 cycles of
460 freeze/thaw.

461 Fig. 8. Relative breakage (B_r) vs Mean Stress (p').

462 Fig. 9. Comparison of B_r values in this study to literature values.

463

464

465 **References**

466 Altuhafi, F. N., and Coop, M. R. (2011) “Changes to particle characteristics associated
467 with the compression of sands.” *Geotechnique*, **61**(6), 459–471. DOI
468 10.1680/geot.9.P.114.

469 ASTM International. (2011). “Standard test method for single pellet crush strength of
470 formed catalysts and catalyst carriers.” *ASTM D 4179-11.*, West Conshohocken, PA,
471 USA.

472 ASTM International (2011). "Standard test method for consolidated drained triaxial
473 compression test for soils." *ASTM D4767-11.*, West Conshohocken, PA, USA.

474 BSI (British Standards Institution). (2016). “Lightweight aggregates.” *BSI BS EN*
475 *13055-4.*, London, UK. Carbon8. <<http://c8a.co.uk/>> (Mar. 07, 2018).

476 Cassini, F., Viggiani, G.M.B., and Springman, S.M. (2013) “Breakage of an artificial
477 crushable material under loading.” *Granular Matter*, **15**(5), 661-673 DOI
478 10.1007/s10035-013-0432-x.

479 Coop, M. (1990). “The mechanics of uncemented carbonate sands.” *Geotechnique*, **40**
480 (4), 607–615.

481 Costa, I., Baciocchi, R., Poletini, A., Pomi, R., Hills, C.D., and Carey, P.J. (2007).
482 “Current status and perspectives of accelerated carbonation processes on municipal
483 waste combustion residues.” *Environmental Monitoring and Assessment*, **135**, 55-75.

484 Domingo, C., Loste, E., Gomez-Morales, J., Garcia-Carmona, J., and Fraile, J. (2006).
485 “Calcite precipitation by a high-pressure CO₂ carbonation route.” *Journal of*

486 *Supercritical Fluids*, **36**(3), 202–215.

487 Fernández, B. M., Simons, S. J. R., Hills, C. D., and Carey, P. J. (2004). “A review of
488 accelerated carbonation technology in the treatment of cement-based materials and
489 sequestration of CO₂.” *Journal of Hazardous Materials*, **112**(3), 193–205.
490 <<http://dx.doi.org/10.1016/j.jhazmat.2004.04.019>>

491 Gunning, P. J., Hills, C. D., and Carey, P. J. (2009). “Production of lightweight
492 aggregate from industrial waste and carbon dioxide.” *Waste Management*, **29**(10),
493 2722–2728. <<http://dx.doi.org/10.1016/j.wasman.2009.05.021>>

494 Gunning, P.J., Hills, C.D., Antemir, A., and Carey, P.J. (2011). “Secondary aggregate
495 from waste treated with carbon dioxide,” *Proc., Institute of Civil Engineers –*
496 *Construction Materials*, 164(5), 231-239. <<https://doi.org/10.1680/coma.1000011>>

497 Hardin, B.O. (1985). “Crushing of soil particles.” *Journal of Geotechnical Engineering*,
498 **111**(10), 1177–1192.

499 Klotz, E. U., and Coop, M. R. (2001). “An investigation of the effect of soil state on the
500 capacity of driven piles in sands.” *Geotechnique*, **51**(9), 733-751.

501 Lade, P.V., Yamamuro, J.A., and Bopp, P.A. (1996). “Significance of particle crushing
502 in granular materials.” *Journal Geotechnical. Engineering American Society of Civil*
503 *Engineers (ASCE)*, **122**(4), 309–316.<[https://doi.org/10.1061/\(ASCE\)0733-](https://doi.org/10.1061/(ASCE)0733-9410(1996)122:4(309))
504 [>](https://doi.org/10.1061/(ASCE)0733-9410(1996)122:4(309))

505 Lake, C.B., Choi, H., Hills, C.D., Gunning, P. and Manaqibwala, I. (2016).
506 “Manufactured Aggregate from Cement Kiln Dust.” *Environmental Geotechnics*,

507 <<http://dx.doi.org/10.1680/jenge.15.00074>>

508 Lee, K. L., and Farhoomand, I. (1967). “Compressibility and crushing of granular soil.”

509 *Canadian Geotechnical Journal*, **4**(1), 68–86. <<http://dx.doi.org/10.1139/t67-012>>

510 Marsal, R. J. (1967). “Large-scale testing of rockfills materials.” *J. Soil Mech. Found.*

511 *Engineering Division. American Society of Civil Engineers (ASCE)*, **93**(2), 27–44.

512 Mun, W., and McCartney, J. S. (2017). “Effective Stress Analysis of the Undrained

513 Compression of Unsaturated Soils.” *19th International Conference on Soil Mechanics*

514 *and Geotechnical Engineering*. Seoul.

515 Shahnazari, H., and Rezvani, R. (2013). “Effective parameters for the particle breakage

516 of calcareous sands: An experimental study.” *Engineering Geology*, **159**, 98-105.

517 <<http://dx.doi.org/10.1016/j.enggeo.2013.03.005>>

518 Shipton, B., and Coop, M. R. (2012). “On the compression behaviour of reconstituted

519 soils.” *Soil and Foundation*. **52**(4), 668-681.

520 <<https://doi.org/10.1016/j.sandf.2012.07.008>>

521 Yamamuro, J. A., and Lade, P. V. (1993). “Effects of strain rate on instability of granular

522 soils.” *Geotechnical Testing Journal*, **16**(3), 304–313.

523 Zheng, W., and Tannant, D. (2016). “Frac sand crushing characteristics and morphology

524 changes under high compressive stress and implications for sand pack permeability.”

525 *Canadian Geotechnical Journal* **53**(9), 1412-1423. <[https://doi.org/10.1139/cgj-2016-](https://doi.org/10.1139/cgj-2016-0045)

526 [0045](https://doi.org/10.1139/cgj-2016-0045)>

527 Zheghal, M. (2009). “The impact of grain crushing on road performance.” *Geotechnical*

528 *and Geological Engineering.* **27**, 549–558.

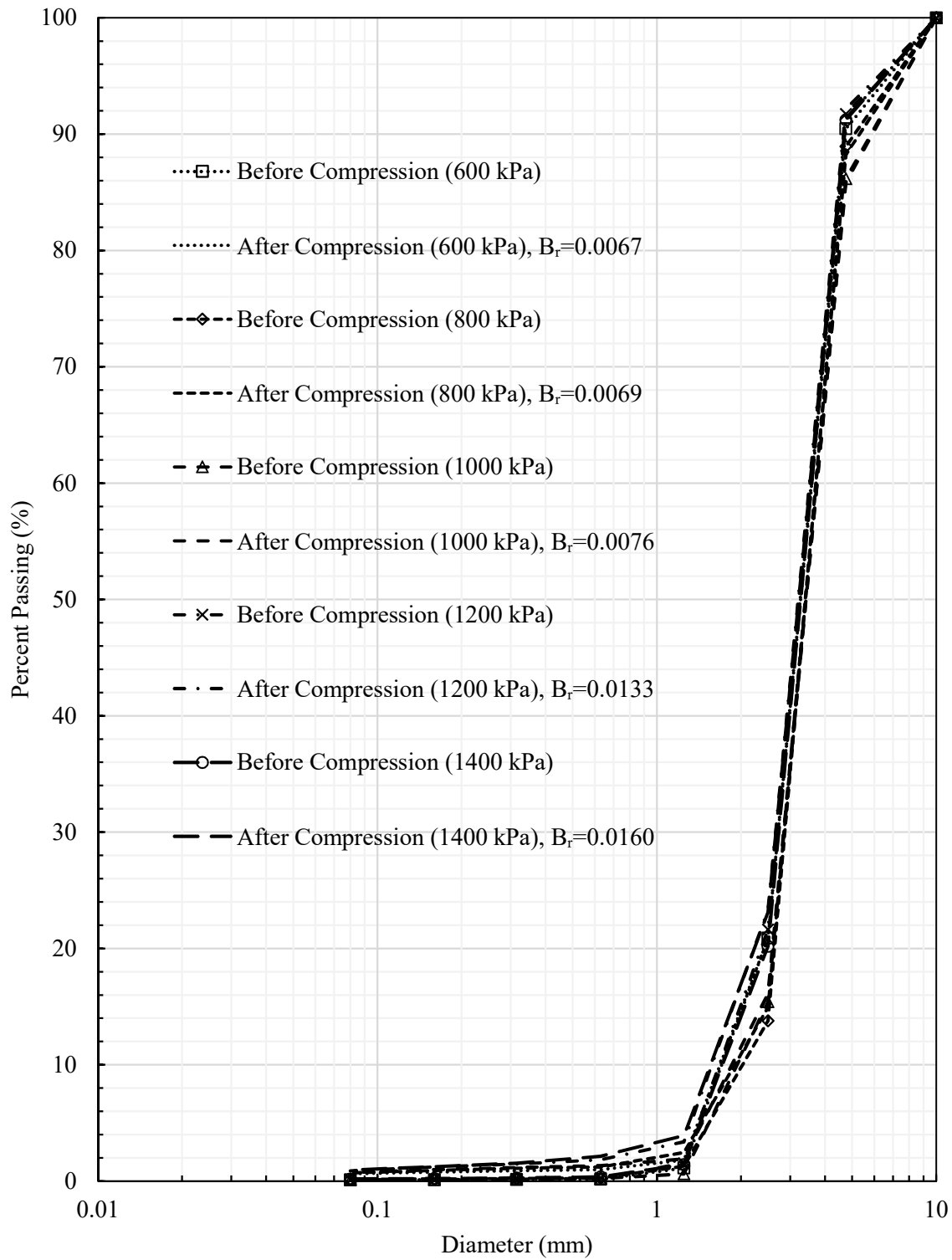


Fig. 1. Particle size distributions for the EPS accelerated carbonated aggregate before and after triaxial compression.

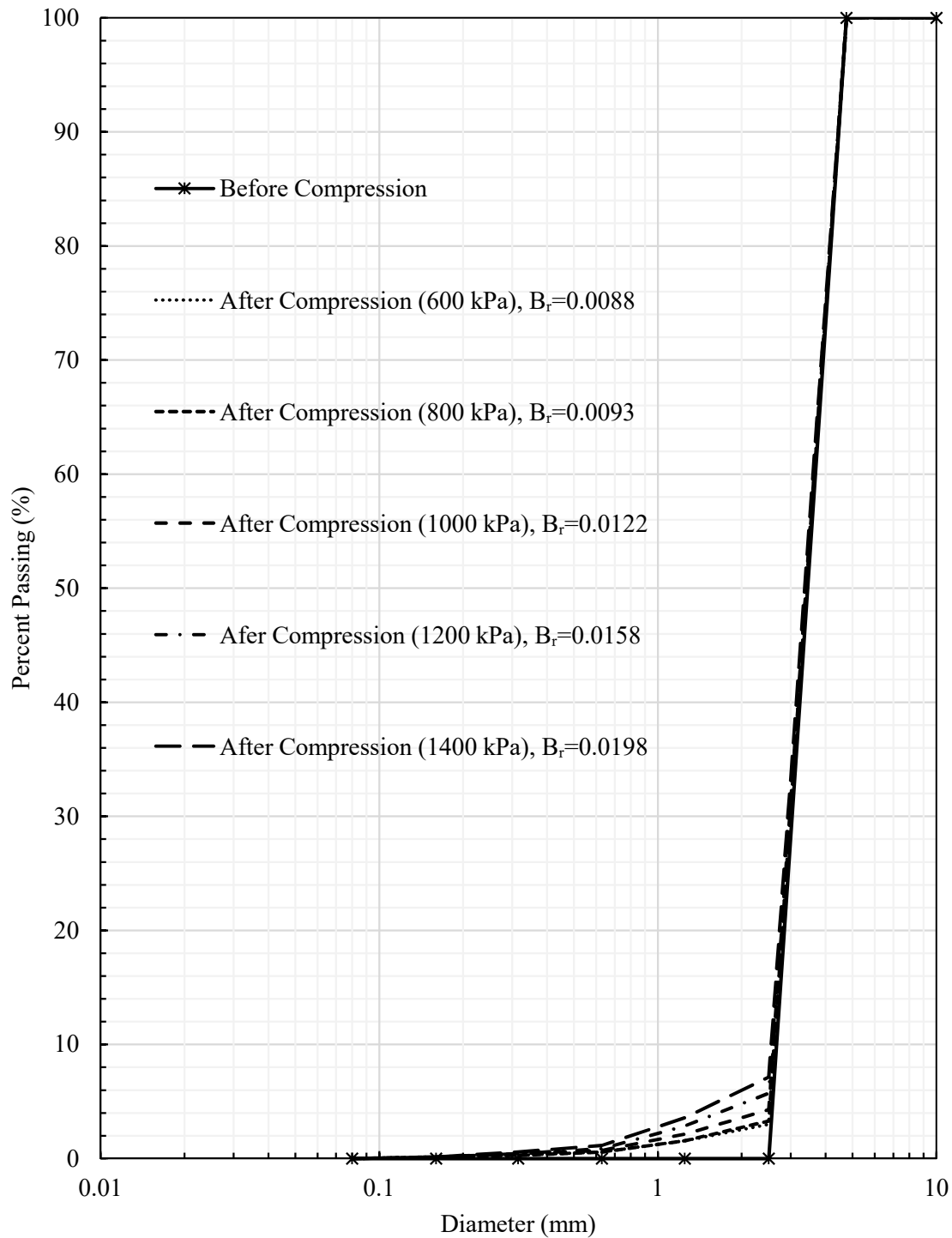


Fig. 2. Particle size distributions for the 5-2.5PS accelerated carbonated aggregate sample before and after triaxial compression.

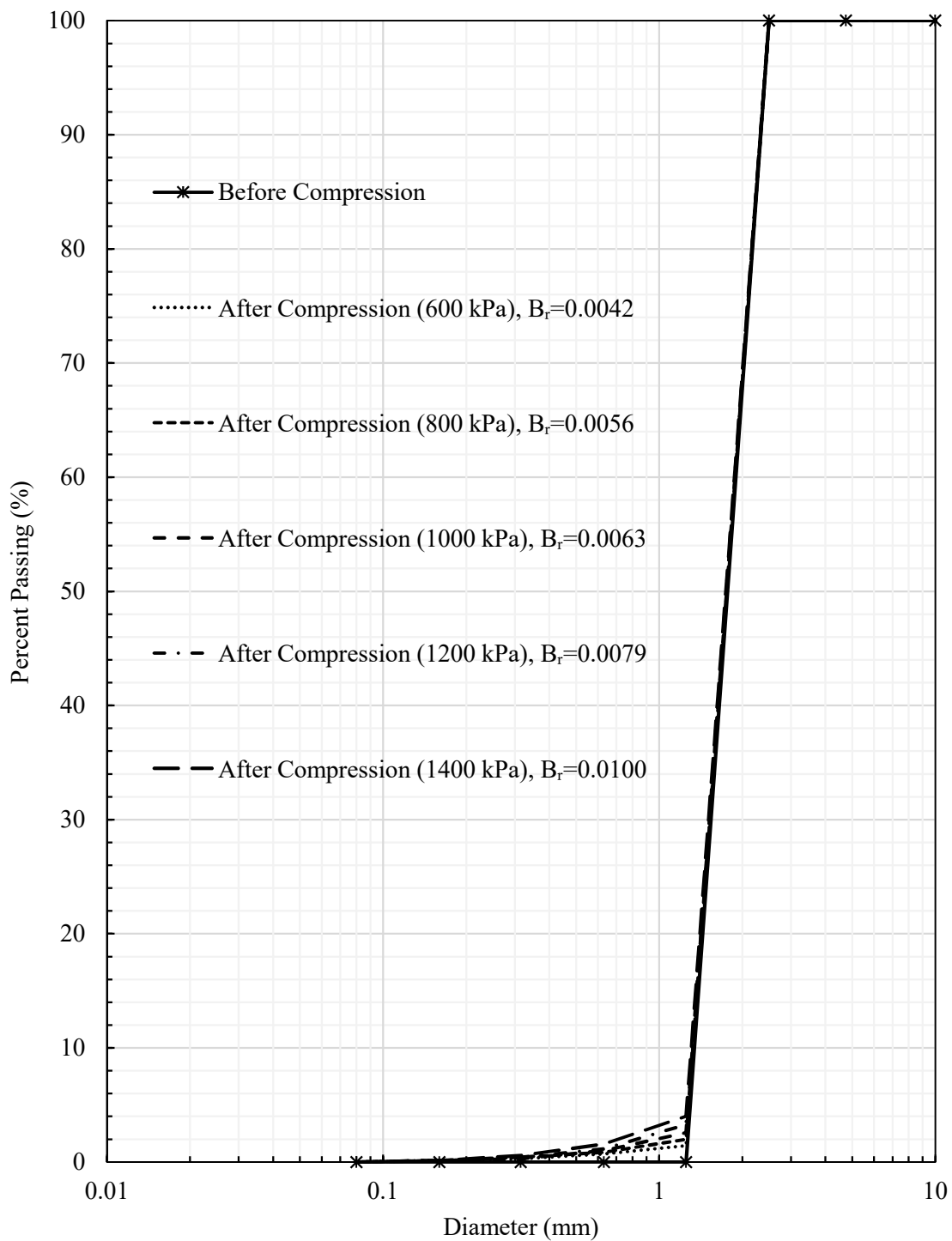


Fig. 3. Particle size distributions for the 2.5-1.25PS accelerated carbonated aggregate sample before and after triaxial compression.

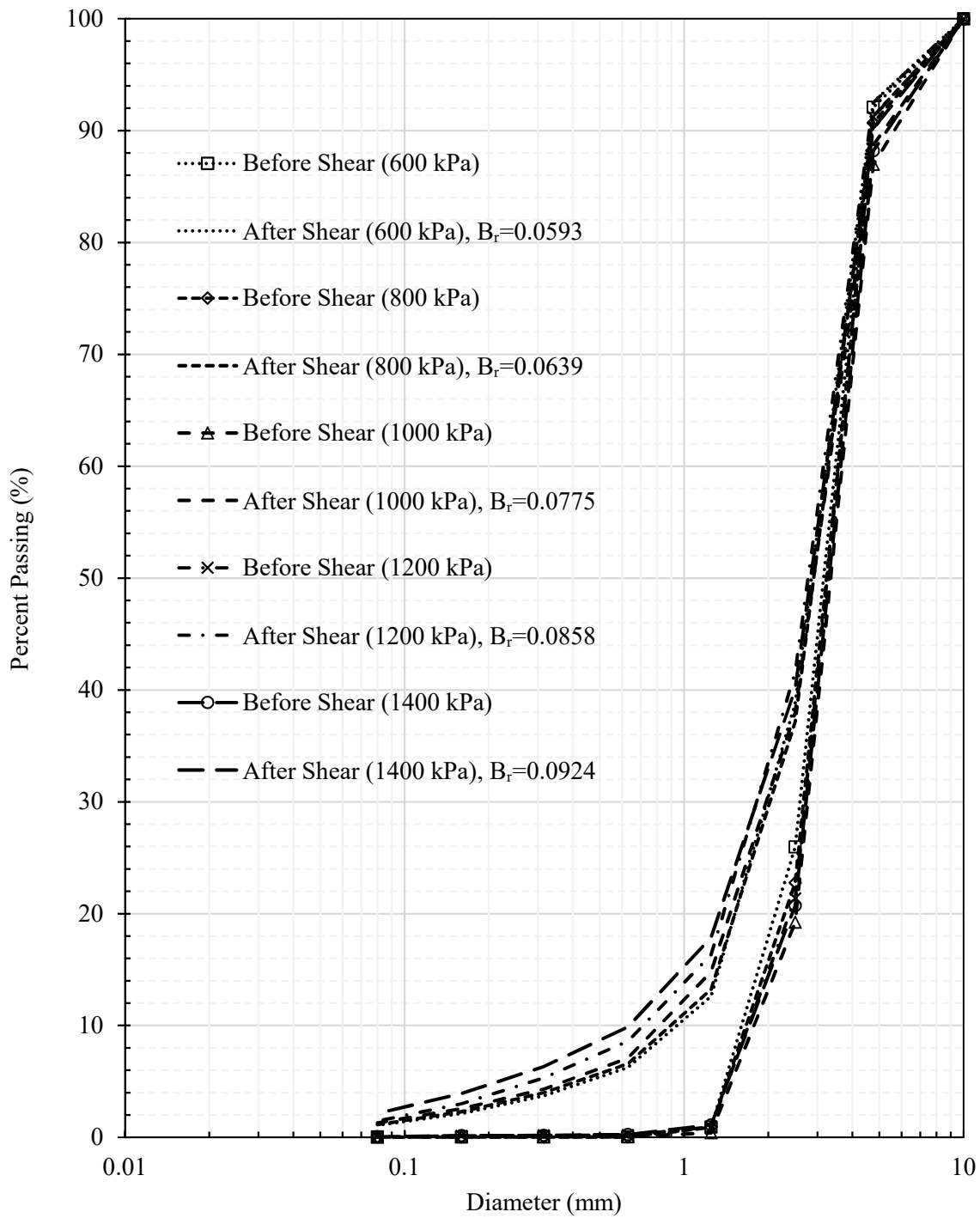


Fig. 4. Particle size distributions for the EPS accelerated carbonated aggregate sample before and after triaxial shear.

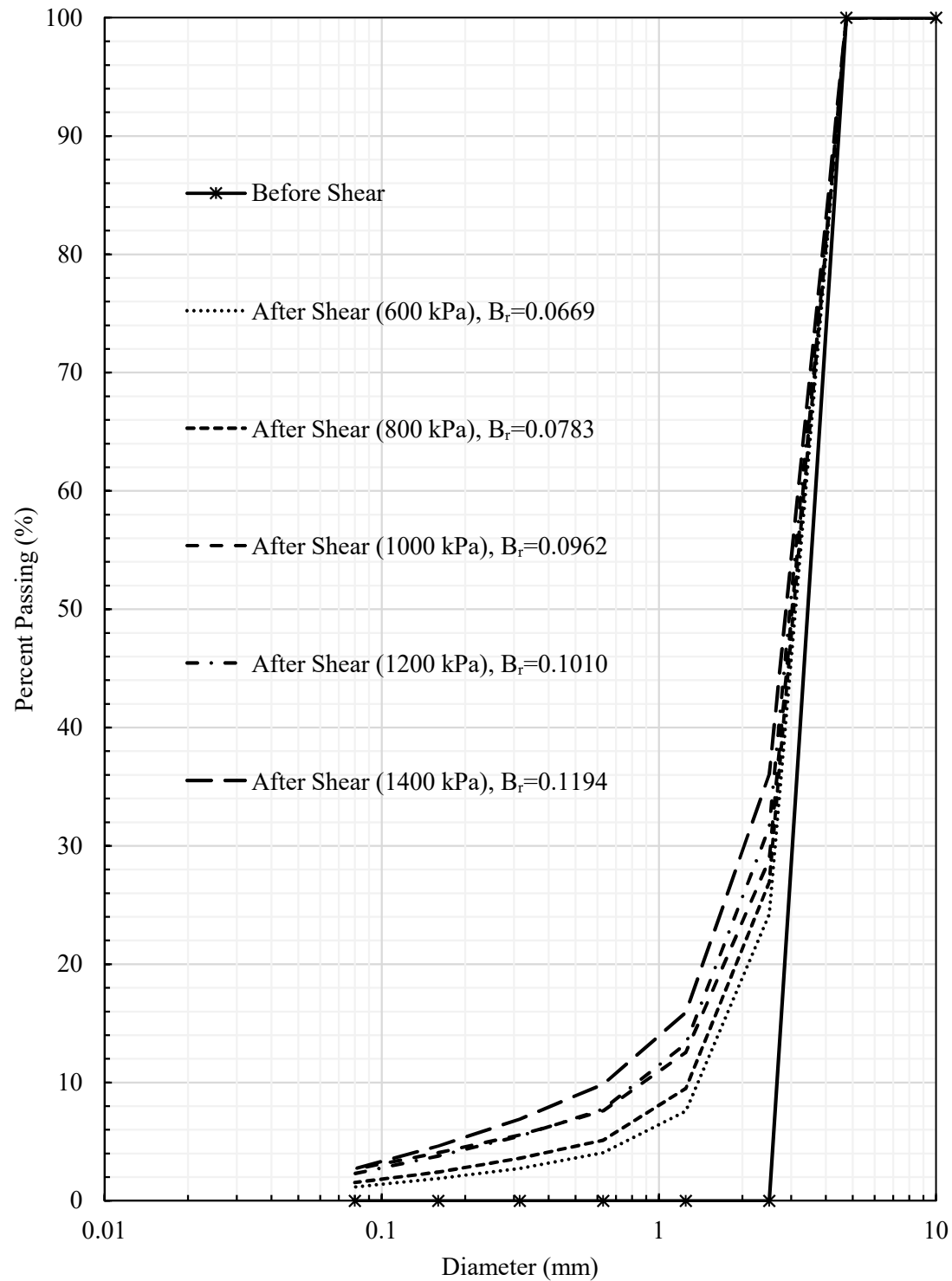


Fig. 5. Particle size distributions for the 5-2.5PS accelerated carbonated aggregate sample before and after triaxial shear.

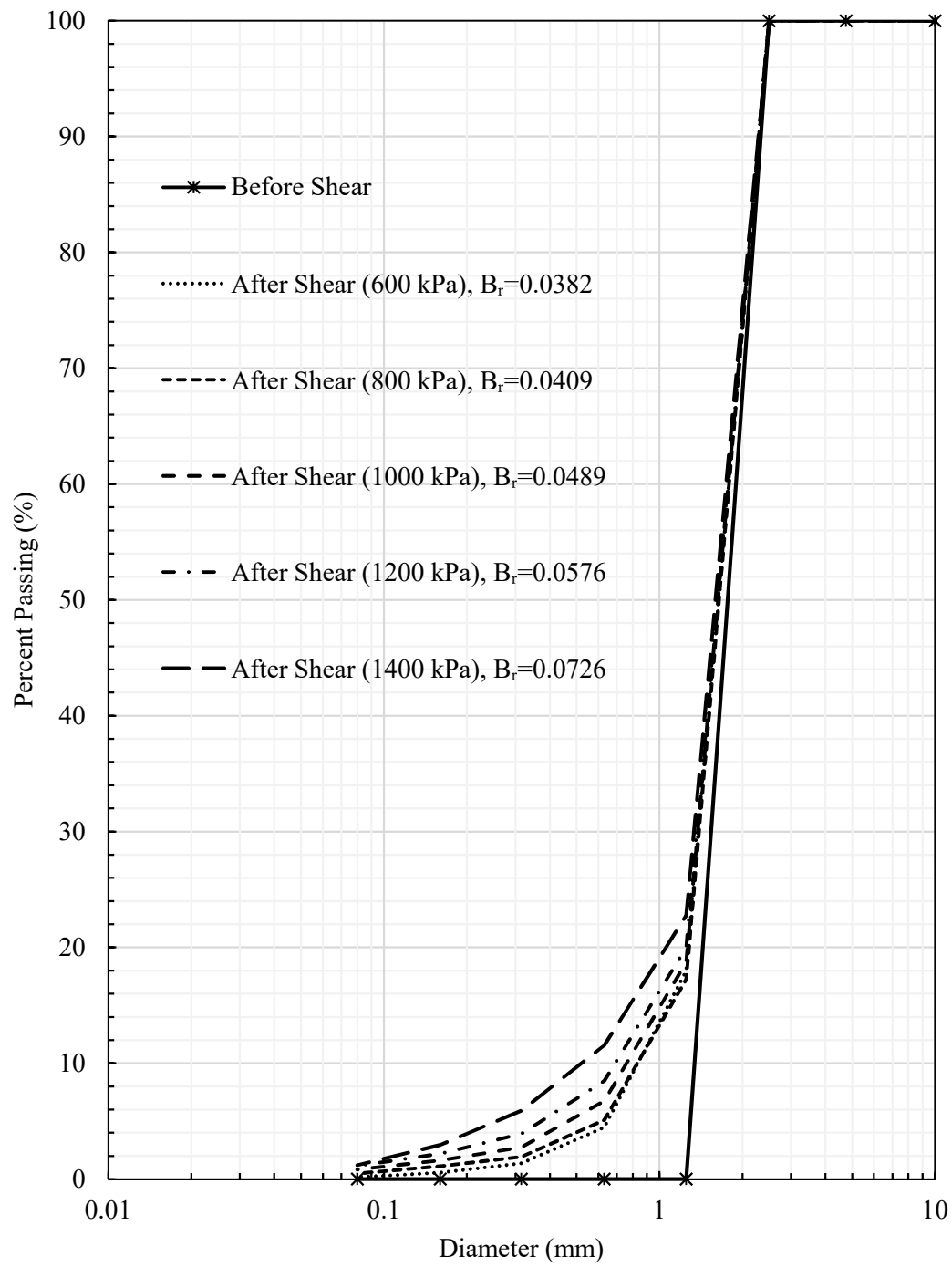


Fig. 6. Particle size distributions for the 1.25-2.5mm size accelerated carbonated aggregate sample before and after triaxial shear.

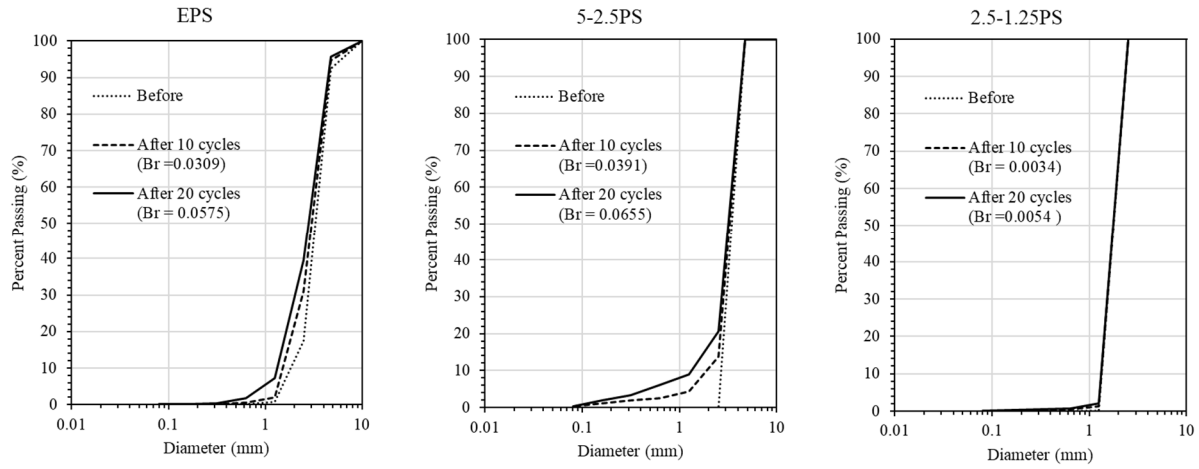


Fig. 7. Accelerated carbonated aggregate particle size distributions, before and after 10 and 20 cycles of freeze/thaw.

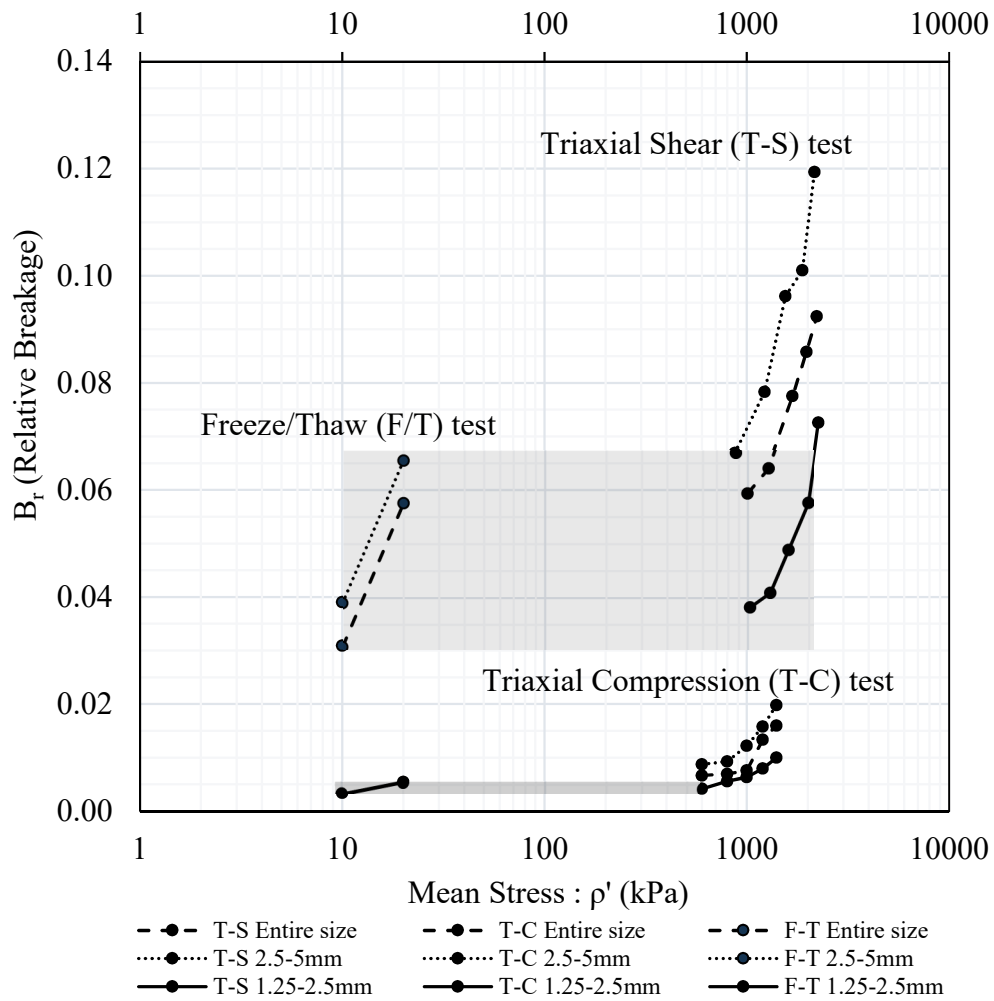


Fig. 8. Relative breakage (B_r) vs Mean Stress (ρ'). Grey shading coincides with the range of B_r values for the 10 and 20 f/t cycles for each particle size. Note: T-C (triaxial compression); T-S (triaxial shear); F/T (Freeze/Thaw)

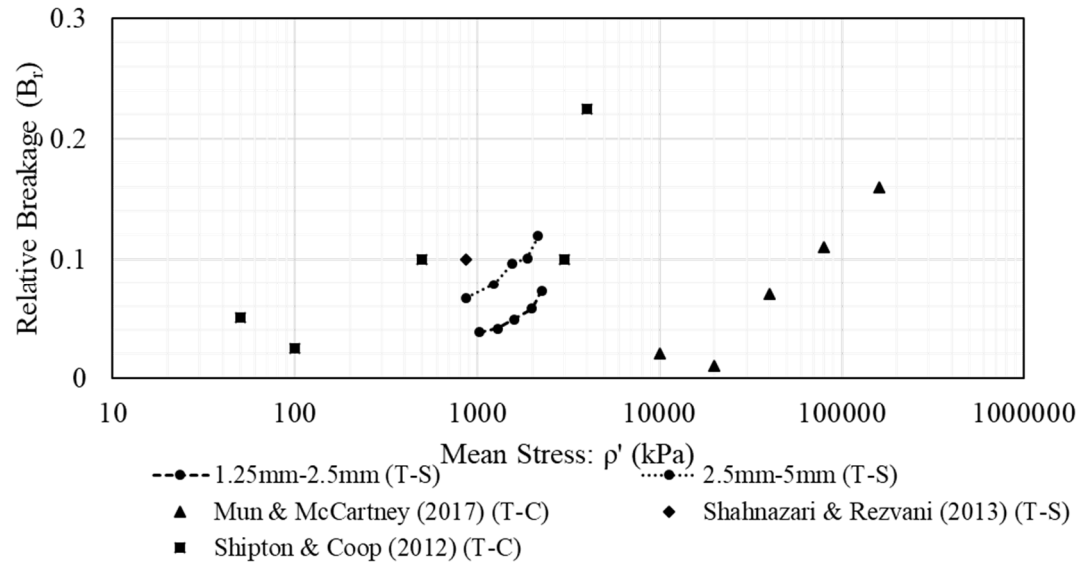


Fig. 9. Comparison of B_r values in this study to literature values.